Fermi National Accelerator Laboratory

FERMILAB-Conf-84/40-T
April, 1984

Possible Cosmological Origin of the Ultra High Energy Cosmic Rays†

CHRISTOPHER T. HILL
Fermi National Accelerator Laboratory
P.O. Box 500, Batavia, Illinois 60510

ABSTRACT

Using improved spectrum evolution results for nucleons propagation through the $3^{\circ}K$ microwave background we present a model of the UHE cosmic rays, above 10^{18}ev, assuming a universal cosmological component associated with bright phase activity and a semi-local component associated with the Virgo cluster. The results for the spectrum and anisotropy are in good agreement with the Haverah Park EAS observations. An unambiguous and potentially detectable electron neutrino spectrum is derived.

---

†Invited Talk, 4th Moriond Astrophysics Meeting, La Plagne, 1984.

Operated by Universities Research Association Inc. under contract with the United States Department of Energy

The possibility that the ultra high energy cosmic rays have an extragalactic, indeed cosmological, origin has long fascinated workers in the field. An expected manifestation would be a Greisen cut-off[1], due to the photoproduction interactions with the $3^{o}K$ microwave background. Others have incorporated the cosmological red-shifting effects[2] and the idea of a bright phase[3] to illustrate how the spectrum above the knee $\sim 10^{16}$ev could arise entirely cosmologically. That the entire spectrum above the knee is cosmological is an extreme point of view which we do not advocate, and can probably be easily refuted by observational evidence, but certainly above 10^{19}ev it is very difficult to understand the anisotropies[4] and the general spectrum shape[5] without a substantial extragalactic component. Also, there is the very interesting corollary production of electron neutrinos[6] which may eventually be detected as upward moving events in the Fly's Eye[7]. The extragalactic source model should be perfected for the forthcoming detailed comparison to experiment as the resource of UHE EAS events increases in the next decade.

Recently we have carefully reanalyzed the spectrum evolution by collisions with the microwave background radiation[8]. We have employed a transport equation approach which is based upon laboratory energy photomeson production data and which we numerically integrate to obtain the spectrum at an arbitrary number of interaction lengths for any given input spectrum. We also compute the induced neutrino spectrum[8,9]. Several new results have emerged from this analysis; most noteable is the appearance of a pile-up of energy degraded nucleons at about 5×10^{19}ev.

The evolution with range of a $1/E^{2.5}$ injection spectrum is shown in Fig.(1). Here one interaction length corresponds to 6Mpc (from 400 γ's/cm^3 and the asymptotic photoproduction cross-section of 120 microbarns) and the figure does not show the inclusion of redshift effects. We do incorporate photomeson production and e^+e^- pair production. The pion differential distribution in arbitrary units is shown in Fig.(2). Through pion decays we ultimately produce electron neutrinos. The asymptotically unit normalized neutrino spectrum is given in Fig.(3). To normalize the neutrino spectrum of Fig.(3) we compute the integrated yield above 10^{18}ev of neutrinos in units of the integrated nucleon spectrum at this energy. These are given in Fig.(4) for different injection indices (we plot 2x the neutrino yield, $c(\gamma,E_0)$, which is the corresponding gamma yield).

These properties of the spectrum evolution are general for a point source neglecting cosmological effects. With them we can construct source models. We consider presently a model containing only extragalactic sources above 10^{18}ev.

We assume sources uniformly distributed throughout a conventional FRW Universe with intrinsic activity increasing as $(1+z)^m$ (m will fit to typically 4, consistent with the increasing activity of QSO's[10] and radio source number counts[11]). The spectrum evolution as shown in Fig.(1) is parameterized as:

$$j(E,E_c) = q(E,E_c)/E^{\gamma_i} \qquad (1)$$

where $q(E,E_c)$ is a homogeneous scale invariant function of the observed energy and cut-off energy E_c. It then follows that the flux observed at present from a distribution of sources up to redshift z' is of the form:

$$j(E)_{diffuse} = \rho_o n_o c H_o^{-1} \int_o^{z'} \frac{(1+z)^{m-1}}{(1+2q_o z)^{1/2}} \, q(E(1+z),\, E_c(1+z)^{-1}) \qquad (2)$$

This convolution must be carried out numerically and normalized numerically. We perform a similar convolution for the neutrino spectrum. We assume deceleration parameter $q_o=1/2$. We define $\Omega_{diffuse} = \rho_o n_o c H_o^{-1}$.

In addition, we assume that the Virgo cluster is atypically close, or brighter and gives an additional contribution to the diffuse one. We write for the Virgo cluster:

$$j_{virgo}(E) = \Omega_{local} q(E,E_c)\Big|_{3i.l.} E^{-\gamma_i} \quad . \qquad (3)$$

We assume a universal injection index independent of the energy and we fit the observed spectrum with γ_i, Ω_{local}, and $\Omega_{diffuse}$.

We find that the best fits occur with $\gamma_i=2.0$ though there are insufficient statistics to bracket this result to within $\pm.5$. The results are shown in Fig.(5). Since the Virgo cluster is not so evolved as the diffuse contributions, it produces a large anisotropy above 10^{19}ev. This is shown from our fit to the spectrum in Fig.(6).

In the spectrum we see two general features: (i) a gentle dip occurs at 10^{19}ev due to the transition from the diffuse component to the Virgo component (this is not the same as the pair production dip seen in Fig.(1)); (ii) an "ankle" at 7×10^{19}ev associated with the flat injection index of the Virgo cluster and the pile-up phenomenon.

We can use our fit to predict the electron neutrino spectrum. This spectrum is flat below $5x10^{18}ev/(1+z')^2$ and above that energy has a universal differential index equal to the nucleon index plus 1/2 (this presumes deceleration parameter of 1/2), hence an index of about 3.5. Above $10^{19}ev$ the spectrum is very weak and is mostly the Virgo component. These results are shown in Fig.(7). These results are within an order of magnitude in intensity and energy from being detected at the Fly's Eye.[7)]

Though our model fit is based upon sparse data and the statistics are poor, we see two general features that are rather striking, the dip and ankle. As further data accrues the persistence of these features may lend credence to the picture outlined here. The acid test would be the discovery of UHE neutrinos, since it is very difficult to imagine competing processes that could lead to such objects.

REFERENCES

1. K.Greisen, Phys.Rev.Lett. 16,748 (1966); V.A.Kuzmin, G.T.Zatsepin. Zh.Eksp.Teor.Fiz., 4,78 (1966).
2. A.M.Hillas, Canadian J. of Phys., 46,5623 (1968); M.Giler et.al. J.Phys.G; Nucl.Phys., 6,1561 (1980); A.Strong et.al., J. Phys. A, Math Nucl. & Gen. 7, 120 (1974).
3. R.Partridge, P.J.E.Peebles Ap.J. 147,868, (1967).
4. J.Linsley, in "The Origin of Cosmic Rays" 53-68 ed. Setti et.al. (1981) and refs. therein.
5. J. Lloyd-Evans et.al. 8th Euro. CR Symposium, Bologna, (1983); Proc. 16th ICRC, Kyoto, 13,130 (1979).
6. F.W.Stecker, Ap.J. 228,919 (1979).
7. P. Sokolsky, Proc. Utah CR Workshop (1983).
8. C.T.Hill and D.N.Schramm, Fermilab-Pub-83/89-THY.
9. C.T.Hill and D.N.Schramm, Phys.Lett. 131B,247 (1983).
10. M.Schmidt, "Stars and Stellar Systems", Vol.IX, G. Kuiper ed., U.of Chicago Press (1975).
11. M.Longair, Monthly Notices R.A.S., 133, 421 (1966).

FIGURE CAPTIONS

Fig. 1: $1/E^{2.5}$ injection at various ranges in interaction lengths. 1 i.l. = 6 Mpc.

Fig. 2: π-differential distribution with range in i.l.

Fig. 3: Electron neutrino differential spectrum with range in i.l.

Fig. 4: 2 × electron neutrino yield with range.

Fig. 5: Best fits to Haverah Park differential spectrum.

Fig. 6: Anisotropy deduced from model fits.

Fig. 7: Predicted ν_e spectrum from best fit, γ_i=2.0, to nucleon spectrum.

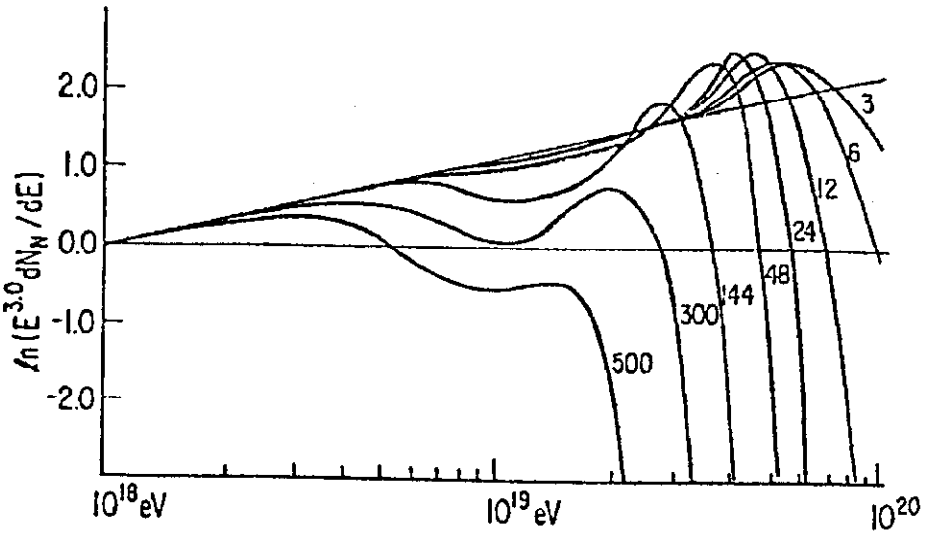

Fig. 1: $1/E^{2.5}$ injection at various ranges in interaction lengths. 1 i.l. = 6 Mpc.

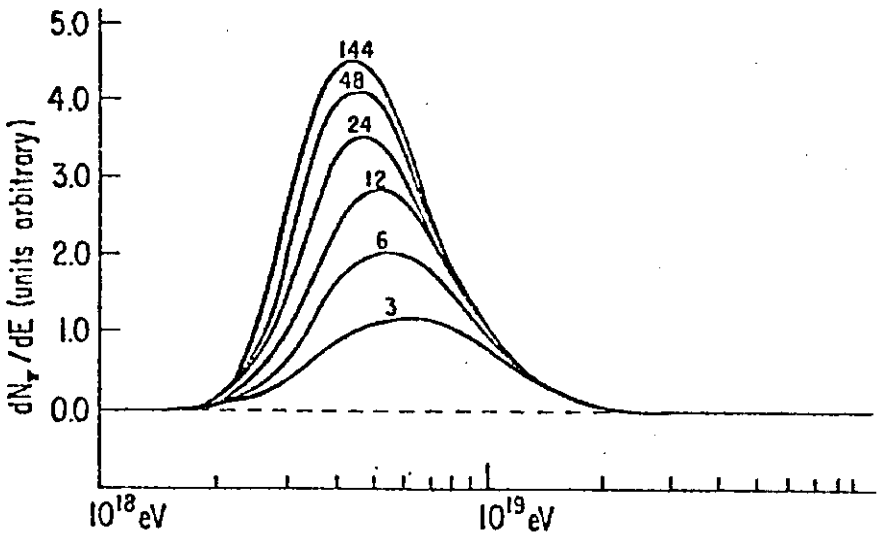

Fig. 2: π-differential distribution with range in i.l.

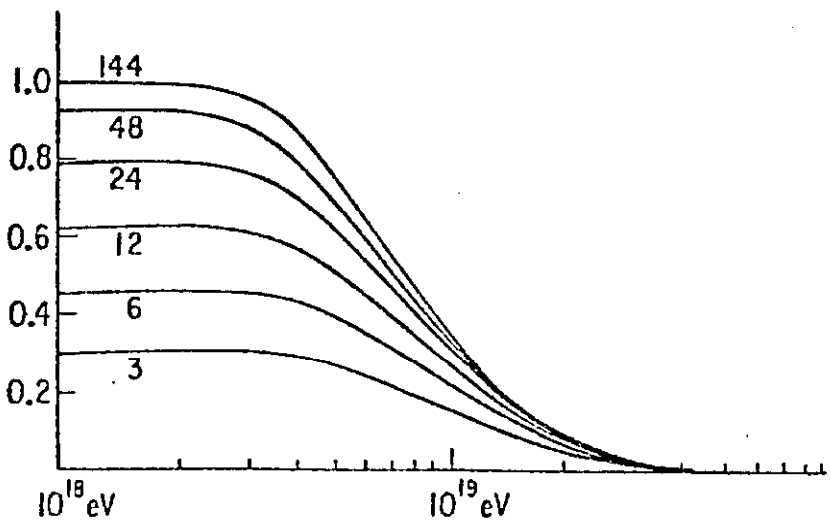

Fig. 3: Electron neutrino differential spectrum with range in i.l.

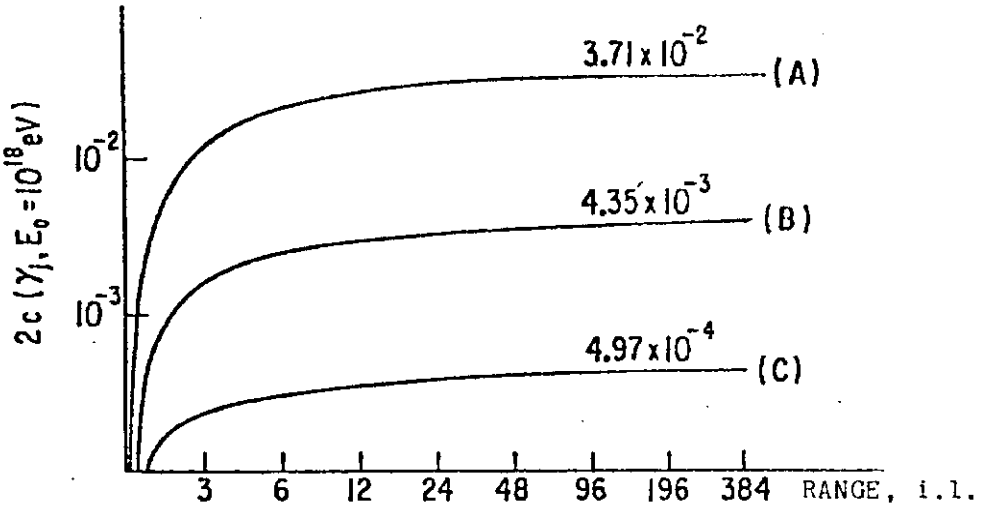

Fig. 4: 2 × electron neutrino yield with range.

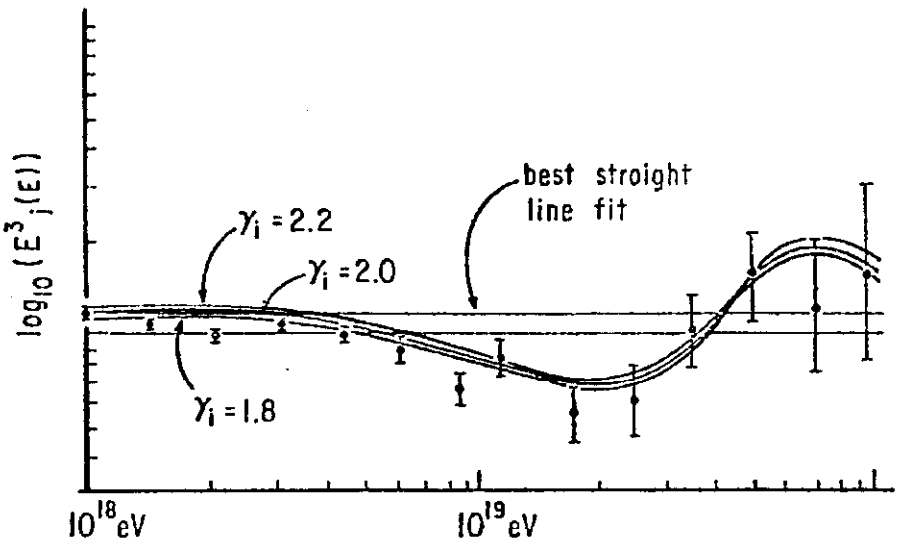

Fig. 5: Best fits to Haverah Park differential spectrum.

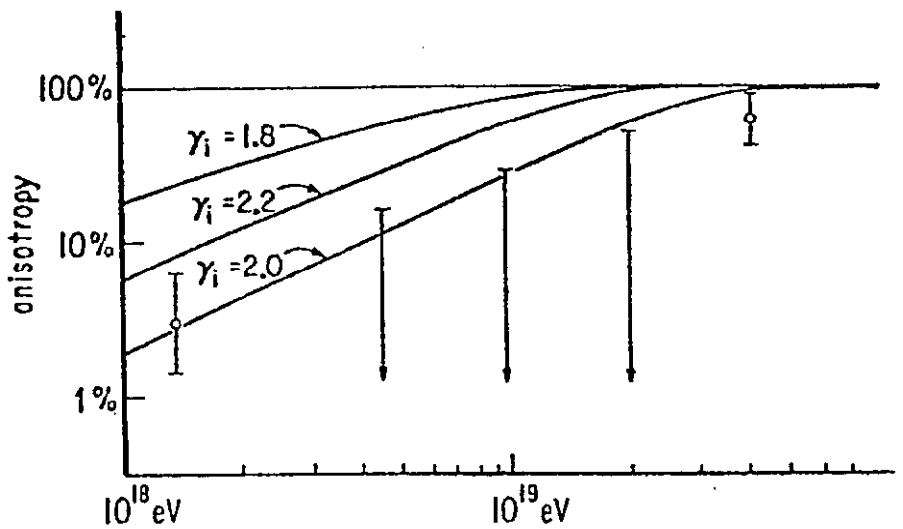

Fig. 6: Anisotropy deduced from model fits.

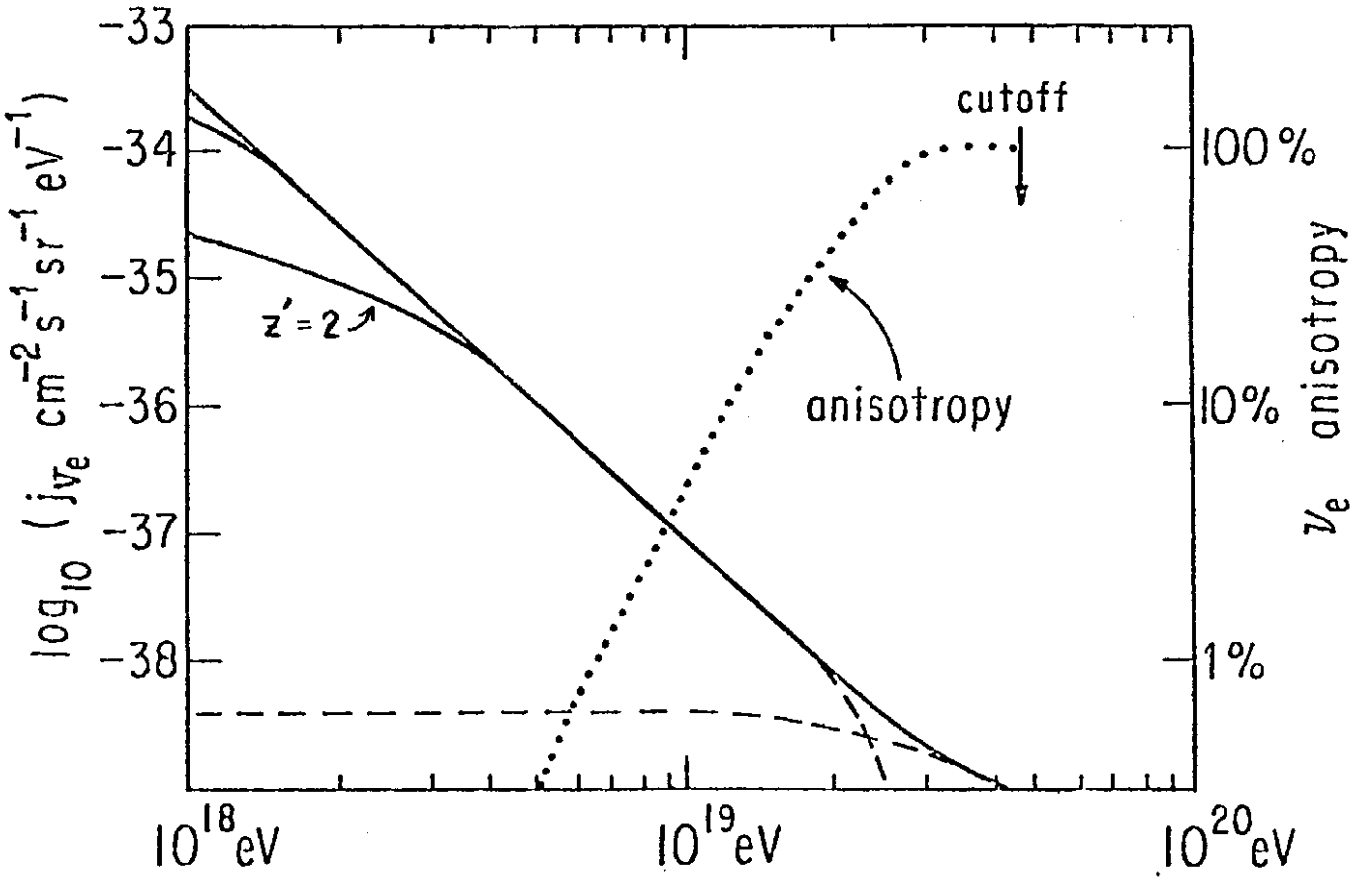

Fig. 7: Predicted ν_e spectrum from best fit, γ_i=2.0, to nucleon spectrum.